NACA RM E54G15

NACA

RESEARCH MEMORANDUM

PUMPING CHARACTERISTICS FOR SEVERAL SIMULATED VARIABLE-GEOMETRY EJECTORS WITH HOT AND COLD PRIMARY FLOW

By John L. Allen

Lewis Flight Propulsion Laboratory
Cleveland, Ohio

NATIONAL ADVISORY COMMITTEE
FOR AERONAUTICS

WASHINGTON

September 8, 1954

NACA RM E54G15

NATIONAL ADVISORY COMMITTEE FOR AERONAUTICS

RESEARCH MEMORANDUM

PUMPING CHARACTERISTICS FOR SEVERAL SIMULATED VARIABLE-GEOMETRY EJECTORS WITH HOT AND COLD PRIMARY FLOW

By John L. Allen

SUMMARY

An investigation was made of the pumping characteristics of eight conical ejectors mounted on a 1/10-scale fuselage portion of a supersonic airplane. The configurations simulated various positions of a two-position nozzle with a fixed shroud and a double-iris exit. Diameter ratio varied from 1.12 to 1.48, and spacing ratio from 0.123 to 0.70, as dictated by variable-geometry considerations. Nozzle pressure ratios from 2.4 to 12 and ejector weight flows from 1 to 15 percent of the nozzle weight flow were investigated.

Variations of flight Mach number from 0 to 2.0 had no significant effect on the internal flow. Differences in pumping characteristics were found when the data were compared with published quiescent-air data for equivalent diameter and spacing ratios. These differences are qualitatively associated with the geometry of the secondary passage and particularly with changes in shroud wall angle. The general trends obtained for changes in diameter and spacing ratio were, however, in agreement. Reasonable agreement was obtained between data at primary-air temperatures of 1200° to 3000° R and data at 600° to 800° R for choked secondary flow and spacing ratios less than 0.5.

Relatively poor ejector pumping characteristics were obtained with the simulated afterburning exits because of concomitant reductions in diameter or spacing ratios for the two types of variable geometry. Free-stream normal-shock pressure recoveries were required for some operating conditions in order to supply secondary air to the ejector by means of an auxiliary inlet.

INTRODUCTION

Increased attention to the use of the ejector in supersonic turbojet aircraft as a pump for supplying cooling air and particularly as a means for replacing the reexpansion portion of the exhaust nozzle has

dictated the need for investigating configurations more typical of contemplated installations. Since turbojet engines equipped with afterburners require a two-position or variable-area exhaust nozzle, ejector diameter or spacing ratios change with the mode of engine operation. In addition, the ejector shroud may be mechanically variable (e.g., an iris nozzle with an iris shroud), and, consequently, the secondary-passage geometry also varies. Therefore, the pumping characteristics of a variable-geometry ejector may not be adequately predicted by means of investigations such as references 1 and 2, wherein the secondary-passage geometry is not an experimental variable. Furthermore, the effects of a supersonic free stream on conical ejectors have not been determined.

Accordingly, a limited investigation of the pumping characteristics of eight conical ejector configurations, each mounted on a 1/10-scale fuselage of a proposed supersonic airplane, has been conducted in the NACA Lewis 8- by 6-foot supersonic tunnel at flight Mach numbers of 0, 0.6, 1.5, 1.7, and 2.0 and angles of attack of zero and 3°. The configurations simulated several positions of two types of variable-geometry exits, specifically a two-position nozzle with a fixed shroud and a double-iris exit. Ejector performance was studied under an actual schedule of operation as simulated by a series of fixed-geometry exits. A range of nozzle pressure and ejector weight-flow ratios was investigated with and without heat addition to the primary flow. Diameter and spacing ratios varied from 1.12 to 1.48 and 0.123 to 0.70, respectively, and the secondary-shroud wall angle varied from 1.5° to 15°. These variations were not in a systematic manner, except as dictated by the variable-geometry requirements.

SYMBOLS

The following symbols are used in this report:

A	area
D	diameter
H	total pressure
M	Mach number
p	static pressure
S	shroud length
T	total temperature

w weight flow, air plus combustion products

τ temperature ratio, T_s/T_p

φ shroud wall angle

ω weight-flow ratio, w_s/w_p

Subscripts:

p primary or nozzle exit

s secondary or ejector

t throat

0 free stream

APPARATUS AND PROCEDURE

Model Installation and Data Reduction

A schematic diagram of the 1/10-scale model installed in the 8- by 6-foot supersonic tunnel is shown in figure 1, and a sketch of the rear portion of the model showing the combustor, the secondary-air passage, and one of the exit configurations is presented in figure 2. The method of supplying air to the model is the same as that described in reference 3. High-pressure air was regulated by the control valve, measured by means of the A.S.M.E. orifice, and ducted to the model through the piping and hollow wing. The total weight flow (air plus fuel) delivered to the model was determined by knowing the air flow and preheater fuel flow and a leakage calibration. Ejector weight flow was found by means of pressure and temperature measurements and a static calibration of the circumferential perforated ring valve that controlled the ejector weight flow. Nozzle weight flow was found by subtracting the ejector weight flow from the total weight flow, the use of a seal-leakage calibration, and by adding the fuel flow supplied to the model combustor for hot-flow data. The ejector weight flow was varied from about 1 to 15 percent of the nozzle weight flow.

The nozzle or primary pressure ratio H_p/p_0 was computed from the known static pressure, temperature, weight flow, area at the beginning of the nozzle contraction (see fig. 2), and the free-stream static pressure. Nozzle pressure ratio was varied from about 2.4 to 12. Forward of the plane of static-pressure measurement in the nozzle (fig. 2), the configuration geometry was made to accommodate the model combustor and

is not representative of an actual installation. Ejector or secondary pressure ratio H_s/p_0 was found by assuming that stagnation conditions were obtained in the secondary chamber forward of the ring valve and by measuring the pressure by means of static-pressure instrumentation. This assumption was substantiated by limited total-pressure instrumentation aft of the ring valve.

The temperature of the air entering the model, which varied from 600° to 800° R, was measured and used as the secondary-air temperature for both hot and cold primary flow. With the model combustor operating, the temperature at the nozzle throat was found by means of continuity relations with the measured static pressure and an iteration process for the ratio of specific heats. This temperature was controlled over a range from 1200° to 3000° R, for which the corresponding range of $\sqrt{\tau}$ was from 0.447 to 0.709. Data obtained without burning in the model are referred to as cold-flow data, and with burning in the model the term hot flow is used.

Ejector Configurations

The eight ejector configurations investigated are shown in figure 3, and the pertinent ratios and dimensions are given in the accompanying tables. The ejectors are identified by diameter ratio followed by spacing ratio and represent various engine operating points on a proposed airplane flight path for the two types of variable-exit geometries. Those ejectors associated with the two-position nozzles are designated by the letter A (fig. 3(a)), and those associated with the double-iris exit (iris-type primary nozzle and iris-shroud) by the letter B (fig. 3(b)). Ejectors A 1.48-0.67 and A 1.13-0.70 simulate a fixed shroud with nozzle areas for operation without and with afterburning, respectively. Ejector A 1.13-0.23 is a modification of A 1.13-0.70 in that the shroud length is reduced. Ejector A 1.24-0.70 is not intentionally related to the others; however, since the nozzle-exit area closely corresponds to that of ejector A 1.48-0.67, it will be considered as a nonafterburning exit. Ejector B 1.16-0.494 is intended for subsonic operation without afterburning, and ejectors B 1.14-0.214 and B 1.12-0.123 represent full afterburning operation for flight Mach numbers of 1.5 and 2.0, respectively, at an altitude of 35,000 feet (fig. 3(b)). As flight Mach number is increased from nonafterburning at subsonic cruise to full afterburning in supersonic flight, the diameter ratio, spacing ratio, and shroud wall angle decrease for these ejectors. At flight Mach number 2.0, ejector B 1.12-0.123 has a convergent-divergent primary nozzle with a reexpansion area of about 8 percent. Ejector B 1.16-0.133, which has a convergent primary nozzle, is an alternate design for B 1.12-0.123 for flight Mach number 2.0.

RESULTS AND DISCUSSION

Ejector Pumping Characteristics

Pumping characteristics of the eight ejectors for both cold and hot flow are presented in figure 4. Data were taken in a manner that does not permit accurate definition of the break-off point; however, the secondary flow is choked for a given weight-flow ratio in the essentially linear portion of the curve where ejector pressure ratio H_s/p_0 increases in nearly a direct proportion with increasing nozzle pressure ratio H_p/p_0 (ref. 4).

Data presented in these figures were obtained at stream Mach numbers of 0, 0.6, and 1.5 to 2.0 and angles of attack of zero and 3°. The data in figures 4(d) and (e) demonstrate that there was no appreciable effect of flight Mach number on the internal ejector performance. This result was previously observed in reference 5 for cylindrical ejectors. The other configurations also showed no Mach number effects, and for this reason Mach number symbols are not shown. Similarly, the data points are not keyed for the two angles of attack, since no effects were evident.

Inasmuch as the ejectors are not systematically related, only a general comparison of trends of the pumping characteristics is possible, since in most cases shroud wall angle changes as diameter and spacing ratio change. For pumping characteristics presented in the form of ejector against nozzle pressure ratio, the configuration having weight-flow lines with the lowest slope is desirable for selected weight-flow and nozzle pressure ratios, since low values of ejector supply pressure will be required.

Comparison of ejectors having spacing ratios of about 0.70 in order of decreasing diameter ratio - that is, A 1.48-0.67 (fig. 4(a)), A 1.24-0.70 (fig. 4(d)), and A 1.13-0.70 (fig. 4(b)) - shows an appreciable increase in the ejector pressure ratio required to pump a selected weight flow (slope of the required weight-flow lines). This trend qualitatively agrees with the results of reference 2. The required increase in ejector pressure ratio for a step change in weight-flow ratio from 0.01 to 0.05 was smallest for ejector A 1.48-0.67 and significantly larger by about the same amount for both A 1.24-0.70 and A 1.13-0.70. This is an effect of diameter ratio and may also be influenced somewhat by the variation of secondary-air entrainment by the viscous primary-jet boundary for the different ejectors. A reduction in spacing ratio 0.70 to 0.123 for a diameter ratio of 1.13 (figs. 4(b) and (c)) with the consequent increase in shroud wall angle from 6° to 13.5°, did not significantly alter the pumping characteristics. Again, this qualitatively agrees with the results of references 1 and 2, which indicated no strong spacing-ratio effects for diameter ratios less than 1.21.

For the B series of configurations, the most pronounced effect of a progressive reduction in spacing ratio and shroud wall angle, for a nearly constant diameter ratio - that is, B 1.16-0.494 (fig. 4(e)), B 1.14-0.214 (fig. 4(f)), and B 1.16-0.133 (fig. 4(h)) - was an appreciable increase in the required ejector pressure ratio for a step increase in weight-flow ratio as operation is changed from B 1.16-0.494 (nonafterburning) to B 1.14-0.214 (afterburning). The ejector with the 8-percent reexpanding nozzle, B 1.12-0.123 (fig. 4(g)), required higher ejector pressure ratios to pump a given weight-flow ratio than the ejector with a convergent nozzle, B 1.16-0.133 (fig. 4(h)), intended for the same flight operating condition. At a weight-flow ratio of about 0.10 and a nozzle pressure ratio of 10, this difference in the required secondary pressure ratio amounted to nearly 10 percent.

Comparison with Previous Results

Where possible, the cold-flow data are compared in figure 5 with data obtained from references 1, 2, and 4 for equivalent diameter and spacing ratios. Some of the reasons that prevent an exact comparison are scale effects, limits of interpolation of the reference data, the vena-contracta effect discussed in reference 5, differences in the place of measurement of the secondary total pressure, and, particularly, differences in the shroud geometry as discussed in reference 6. The conical ejectors A 1.13-0.70, A 1.24-0.70, and B 1.16-0.494 did not have choked secondary flow at a nozzle pressure ratio of 3.5 and hence exhibit pumping characteristics somewhat different from the reference conical ejectors. This change in pumping characteristics is attributed to a difference in secondary-passage geometry, which is primarily due to the difference in shroud wall angle between the reference ejectors (8°) and those tested herein (fig. 3). Consequently, the change in momentum of the secondary flow from the primary exit to the shroud exit is not equal for the two cases, and in addition the entrainment of secondary air is altered. Data for ejector B 1.16-0.133, which has a shroud wall angle of only 1.5°, do agree with the cylindrical shroud data of reference 4.

Comparison of Data for Cold and Hot Primary Flow

Cross plots of pumping characteristics for cold and hot flow in the form of the ratio of ejector to nozzle total pressure against temperature-compensated weight-flow ratio for various nozzle pressure ratios are presented in figure 6. In general, the addition of heat to the primary flow necessitated a somewhat higher ejector pressure ratio to pump equivalent weight-flow ratios for a given nozzle pressure ratio. For nozzle pressure ratios near those for choked secondary flow, the hot- and cold-flow data were reasonably correlated for the shorter-spacing-ratio ejectors. The largest disagreement occurred at weight-flow ratios greater than 0.05 for the two largest-spacing-ratio ejectors, A 1.13-0.70 and A 1.24-0.70, probably as a result of mixing or heat transfer,

or both, for the hot case. Burning within the shroud due to incomplete combustion of the primary flow could have occurred for any of the ejectors, and this effect would probably be greatest for the larger-spacing-ratio ejectors. A similar lack of correlation between hot- and cold-flow data for cylindrical shroud ejectors was found in references 7 and 8 as spacing ratio was increased for certain values of diameter ratio. However, somewhat better correlation was obtained for ejector A 1.48-0.67, which has a nearly equal spacing ratio and a larger diameter ratio. Although the data are limited to weight-flow ratios less than 0.06, equal or better correlation might be anticipated at higher values of weight-flow ratio. To some degree, these results substantiate those of reference 8, which indicate that for a given spacing ratio the weight-flow-ratio discrepancy due to heat addition may be large for small diameter ratios but will become smaller as diameter ratio is increased.

Weight-flow-ratio discrepancies due to heat addition, such as those shown for ejectors A 1.13-0.70 and A 1.24-0.70, appear large if interpreted in terms of weight-flow ratio for a constant pressure ratio H_s/H_p. For example, ejector A 1.13-0.70 at H_s/H_p of 0.4 and H_p/p_0 of 6 indicates a weight-flow-ratio reduction of about 25 percent from cold to hot flow; however, ejector total pressure H_s would have to be increased only 8 percent for the hot flow to provide a weight-flow ratio equal to that for cold flow. Inasmuch as the primary temperature varied between 1200° and 3000° R, it is not possible to attribute differences quantitatively between hot and cold data to the effect of changes in specific-heat ratio of the primary flow, as discussed in reference 9 for cylindrical ejectors.

Ejector Air-Supply Requirements

An assumed schedule of turbojet nozzle pressure ratios with and without afterburning, including allowances for inlet losses, is shown in figure 7. Ejector air-supply requirements are shown in figure 8 for the various configurations in the form of the ratio of ejector to nozzle total pressure for the assumed flight and engine conditions. Weight-flow ratios of 0, 0.05, and 0.10 were obtained by cross-plotting the ejector data. For nearly all the ejectors, the ratio of secondary to primary total pressure for a given weight-flow ratio decreased as flight Mach number increased. This change occurs because ejector pressure ratio does not increase as rapidly because of ram as does nozzle pressure ratio for the ejectors considered herein. Superimposed on the plots are lines of constant secondary pressure recovery H_s/H_0, which are indicative of the total-pressure recovery that would have to be supplied to the secondary chamber (such as by means of an auxiliary inlet) to enable the ejector to pump a desired weight-flow ratio (greater than zero). Other methods of supplying secondary air are not considered. For the nonafterburning ejector, A 1.48-0.67, at an altitude of 35,000 feet an ejector supply pressure recovery varying from

about 0.80 to 0.35 is needed for a weight-flow ratio 0.05 as flight Mach number is increased from 0.6 to 1.5. As a result of the change in diameter ratio that occurs as the nozzle is opened to the afterburning position with the shroud remaining fixed, the required supply total-pressure recoveries for ejector A 1.13-0.70 are increased to 0.90 at Mach 0.6 and to 0.60 at Mach 1.5. For the afterburning A-series ejectors, reducing the spacing ratio from that of ejector A 1.13-0.70 to that of ejector A 1.13-0.23, with the consequent increase in shroud wall angle from 6° to 13.5°, reduced the pressure-recovery requirements only slightly. For the nonafterburning A-series ejectors, higher pressure recoveries were required in order to pump equal weight flows for ejector A 1.24-0.70 than for ejector A 1.48-0.67, particularly at a flight Mach number of 1.5.

The double-iris exit simulated by ejectors B 1.16-0.494, B 1.14-0.214, and B 1.12-0.123 indicates a rapid increase in supply pressure-recovery requirements as operation is changed from ejector B 1.16-0.494 to B 1.14-0.214 (fig. 8(b)). This increase is primarily associated with the decreased spacing ratio for the first afterburning position, although diameter ratio, shroud wall angle, and nozzle pressure ratio change slightly. A further reduction in spacing ratio, B 1.14-0.214 to B 1.12-0.123, results in a decrease in the required supply pressure due to ram effects and the change in ejector pumping characteristics. The schedule of diameter and spacing ratios herein is probably not optimum, and an additional degree of freedom, such as a schedule of shroud translation with nozzle-exit area, may improve the variable-geometry pumping characteristics. However, other factors such as simplicity, weight, cooling requirements, net thrust gains, and so forth, must also be considered in the selection of the type of variable geometry.

Although limited by the range of the data, the performance of the various ejectors at sea level indicates that weight-flow ratios of 0.10 are attainable from the free stream at total-pressure recoveries between 0.75 and 1.0 except for ejectors A 1.13-0.23 and B 1.14-0.214. If recoveries greater than 1.0 are required, compressor bleed-off or some other source of high-energy air would be needed.

With respect to cooling, the types of variable-geometry ejectors simulated herein had relatively poor pumping characteristics for the afterburning nozzle positions because of reductions in diameter or spacing ratios from the nonafterburning positions. Assuming the use of turbine-exit air for internal cooling of the afterburner (a perforated antiscreech afterburner cooling liner such as in ref. 10, e.g.), weight-flow ratios on the order of 0.05 are normally required for cooling between the external skin of the afterburner and the airframe. The scoop-type inlet reported in reference 11, which was immersed in fuselage boundary layer, would provide pressure recoveries at critical inlet flow sufficient only for weight-flow ratios of 0.01 to 0.03 for the afterburning A- and B-

series ejectors at Mach numbers from 1.5 to 2.0. This type inlet is, however, potentially capable of somewhat better performance. If weight-flow ratios of 0.10 or higher were required to obtain peak net thrust, for example, an inlet capable of at least normal-shock pressure recovery would be needed for some conditions.

Once the type, size, and location of a fixed-geometry auxiliary inlet is selected to provide a desired weight flow at some flight condition, the inlet operation is effectively a slave of the schedules of nozzle pressure ratio and ejector geometry at other points in the flight plan. A matching problem, therefore, exists for the auxiliary inlet if a desired weight-flow schedule is to be provided with minimum drag penalties at off-design operating conditions.

SUMMARY OF RESULTS

The pumping characteristics of eight conical ejectors having diameter ratios from 1.12 to 1.48 and spacing ratios from 0.123 to 0.70 were investigated at flight Mach numbers of 0, 0.6, 1.5, 1.7, and 2.0. Nozzle pressure ratio was varied from 2.4 to 12, weight-flow ratio from 0.01 to 0.15, and primary-air temperature from 600° to 3000° R. The ejectors were related so that various positions of a two-position nozzle with a fixed shroud and a double-iris exit were simulated. The following results were obtained:

1. No significant effects of flight Mach number or angle of attack on the internal flow were observed.

2. The general trends of the data for changes in diameter and spacing ratio agreed with previously reported quiescent-air data. A detailed comparison with previously reported data for equivalent diameter and spacing ratios indicated a change in pumping characteristics that is presumably related to differences in secondary-passage geometry, primarily due to nonequal shroud wall angles.

3. Reasonable agreement was obtained between the hot- and cold-flow data for choked secondary flow at spacing ratios less than 0.5 when the usual temperature-compensated weight-flow ratio was used.

4. Configurations simulating afterburning positions had relatively poor pumping characteristics, primarily because of a reduction in diameter ratio for the two-position fixed-shroud exit and because of a reduction in spacing ratio and shroud wall angle for the double-iris exit.

5. For some conditions an auxiliary inlet at least capable of normal-shock pressure recoveries was necessary in order for the ejector to pump sufficient secondary air.

Lewis Flight Propulsion Laboratory
National Advisory Committee for Aeronautics
Cleveland, Ohio, July 15, 1954

REFERENCES

1. Greathouse, W. K., and Hollister, D. P.: Preliminary Air-Flow and Thrust Calibrations of Several Conical Cooling-Air Ejectors with a Primary to Secondary Temperature Ratio of 1.0. I - Diameter Ratios of 1.21 and 1.10. NACA RM E52E21, 1952.

2. Greathouse, W. K., and Hollister, D. P.: Preliminary Air-Flow and Thrust Calibrations of Several Conical Cooling-Air Ejectors with a Primary to Secondary Temperature Ratio of 1.0. II - Diameter Ratios of 1.06 and 1.40. NACA RM E52F26, 1952.

3. Hearth, Donald P., and Gorton, Gerald C.: Investigation of Thrust and Drag Characteristics of a Plug-Type Exhaust Nozzle. NACA RM E53L16, 1954.

4. Kochendorfer, Fred D., and Rousso, Morris D.: Performance Characteristics of Aircraft Cooling Ejectors Having Short Cylindrical Shrouds. NACA RM E51E01, 1951.

5. Gorton, Gerald C.: Pumping and Drag Characteristics of an Aircraft Ejector at Subsonic and Supersonic Speeds. NACA RM E54D06, 1954.

6. Huntley, S. C., and Yanowitz, Herbert: Pumping and Thrust Characteristics of Several Divergent Cooling-Air Ejectors and Comparison of Performance with Conical and Cylindrical Ejectors. NACA RM E53J13, 1954.

7. Wilsted, H. D., Huddleston, S. C., and Ellis, C. W.: Effect of Temperature on Performance of Several Ejector Configurations. NACA RM E9E16, 1949.

8. Greathouse, W. K.: Preliminary Investigation of Pumping and Thrust Characteristics of Full-Size Cooling-Air Ejectors at Several Exhaust-Gas Temperatures. NACA RM E54A18, 1954.

9. Kochendorfer, Fred D.: Effect of Properties of Primary Fluid on Performance of Cylindrical Shroud Ejectors. NACA RM E53L24a, 1954.

10. Harp, James L. Jr., Velie, Wallace W., and Bryant, Lively: Investigation of Combustion Screech and a Method of Its Control. NACA RM E53L24b, 1954.

11. Pennington, Donald B., and Simon, Paul C.: Internal Performance at Mach Numbers to 2.0 of Two Auxiliary Inlets Immersed in Fuselage Boundary Layer. NACA RM E53L28b, 1954.

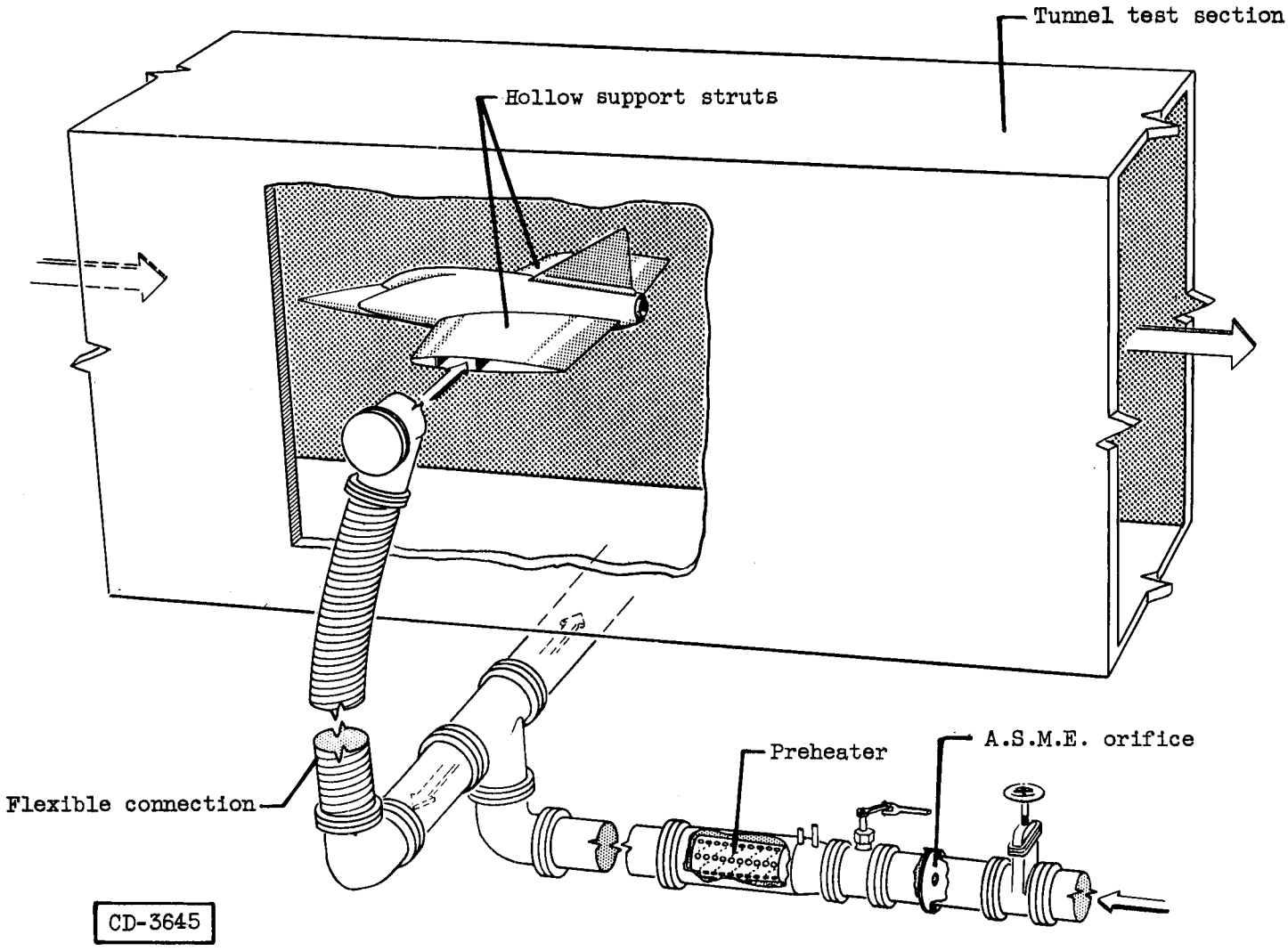

Figure 1. - Schematic drawing of jet-exit model installed in 8- by 6-foot supersonic tunnel.

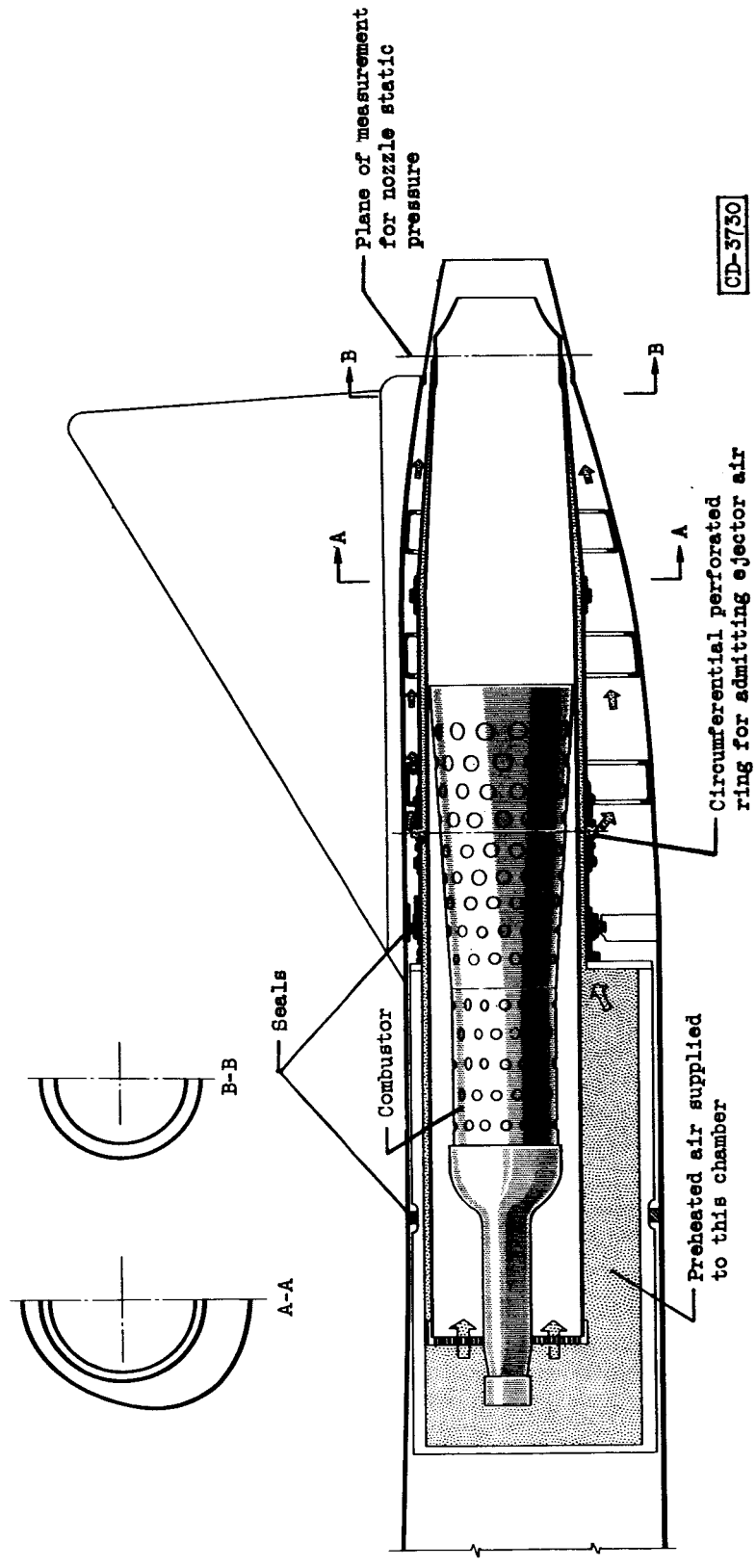

Figure 2. - Schematic diagram of aft portion of 1/10-scale model.

A 1.48-0.67

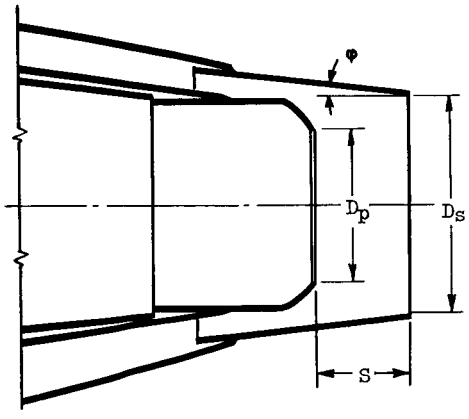

A 1.13-0.23

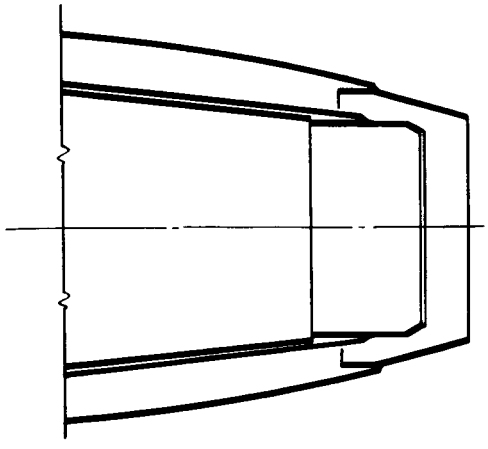

A 1.13-0.70

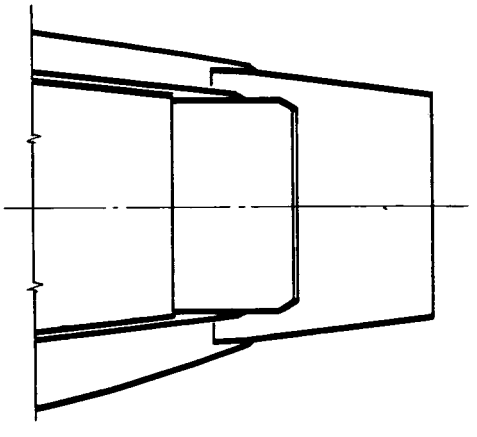

A 1.24-0.70

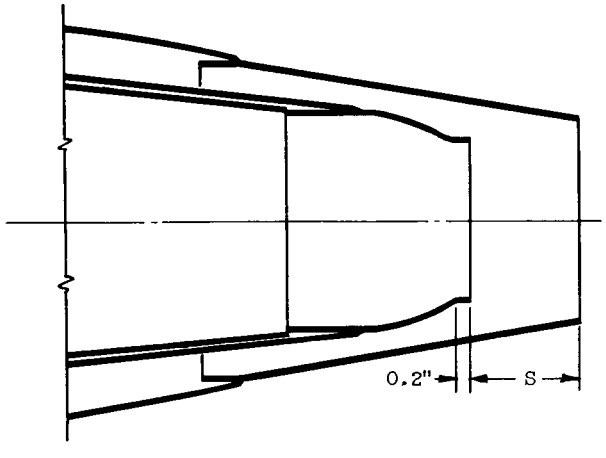

CD-3731

Designation	D_s/D_p	S/D_p	D_p, in.	Shroud wall angle, φ, deg	Design T_p, °R
A 1.48-0.67*	1.48	0.67	2.10	6	1400
A 1.13-0.70*	1.13	0.70	2.75	6	3500
A 1.13-0.23	1.13	0.23	2.75	13.5	3500
A 1.24-0.70	1.24	0.70	2.21	9	1400

* Related ejectors for fixed-shroud, two-position variable-geometry exit.

(a) Two-position convergent nozzle.

Figure 3. - Ejector configurations.

B 1.16-0.494

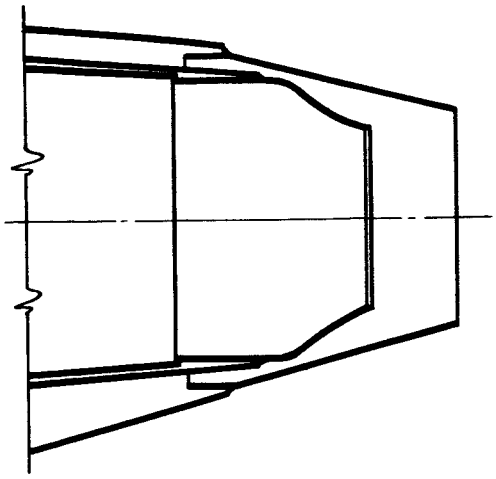

B 1.12-0.123

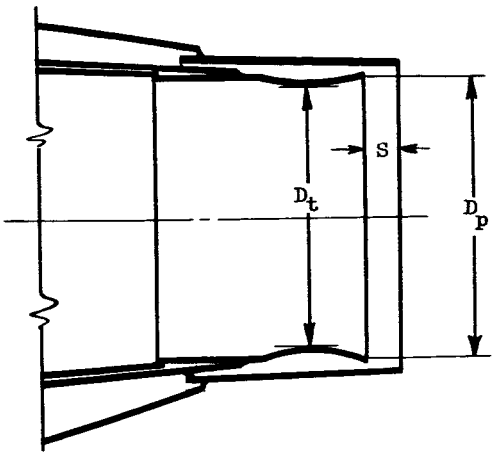

B 1.14-0.214

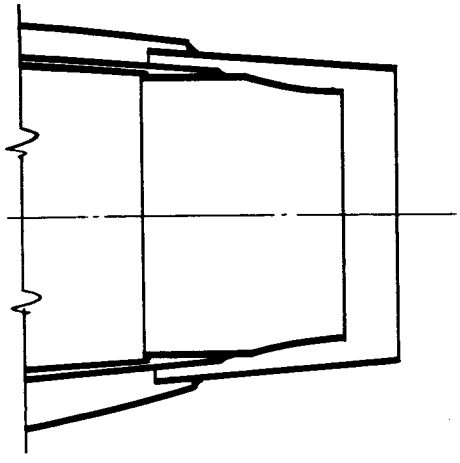

B 1.16-0.133

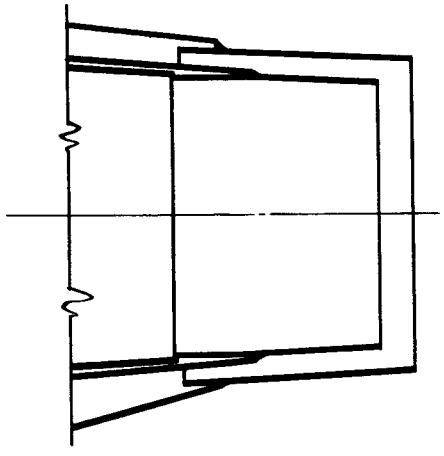

CD-3732

Designation	D_s/D_p	S/D_p	D_p, in.	A_p/A_t	Shroud wall angle, φ, deg	Design	
						M_0	T_p, °R
B 1.16-0.494*	1.16	0.494	2.35	1.0	15	0.6	1400
B 1.14-0.214*	1.14	0.214	3.41	1.0	4.5	1.5	3500
B 1.12-0.123*	1.12	0.123	3.75	1.077	1.5	2.0	3500
B 1.16-0.133	1.16	0.133	3.60	1.0	1.5	2.0	3500

*Related ejectors for double-iris variable-geometry exit.

(b) Continuously variable-area nozzle.

Figure 3. - Concluded. Ejector configurations.

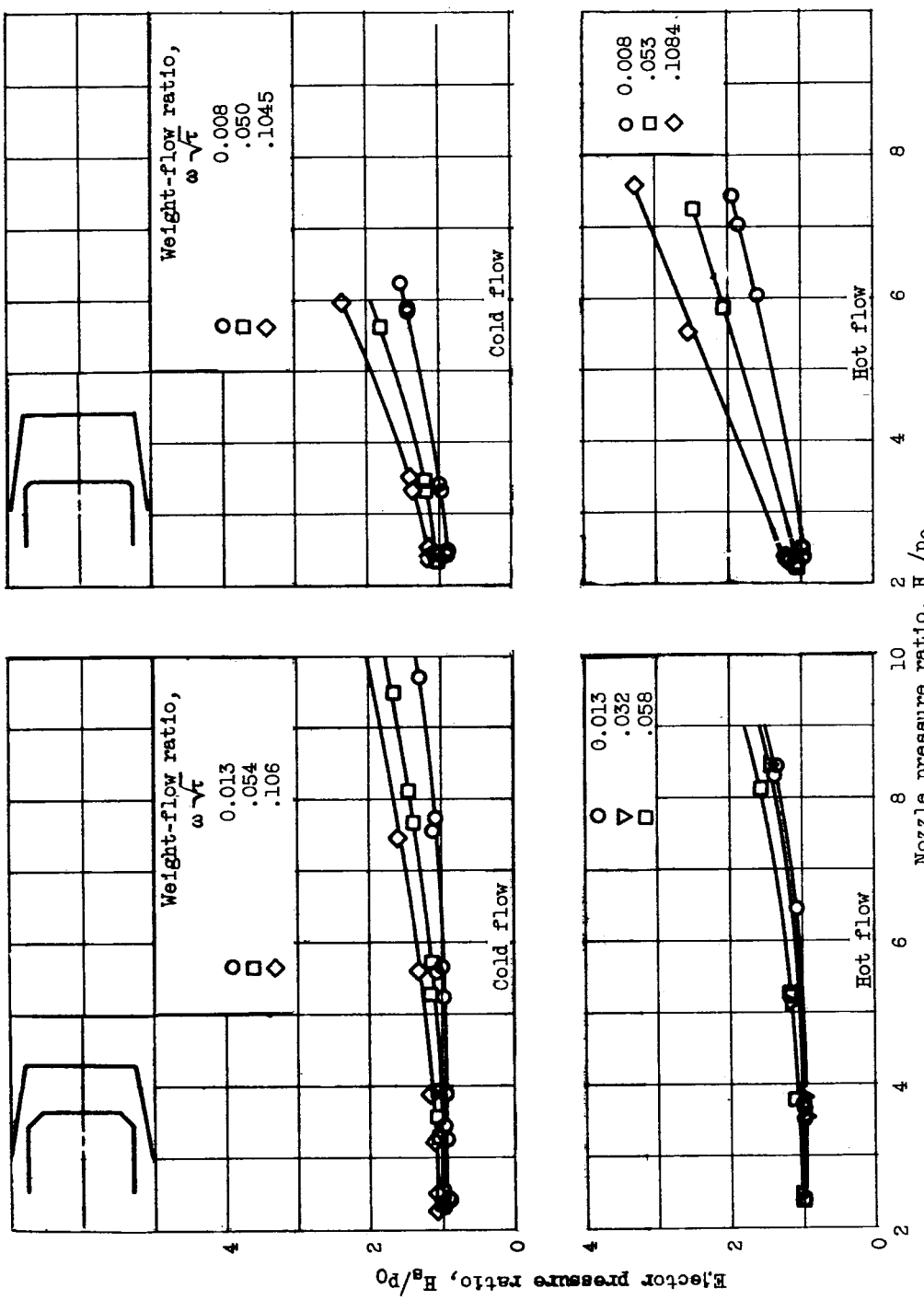

(a) Configuration A 1.48-0.67. Flight Mach numbers, 0, 0.63, 1.5, and 1.7.

(b) Configuration A 1.13-0.70. Flight Mach numbers, 0, 0.62, 1.5, and 1.7.

Figure 4. - Ejector pumping characteristics.

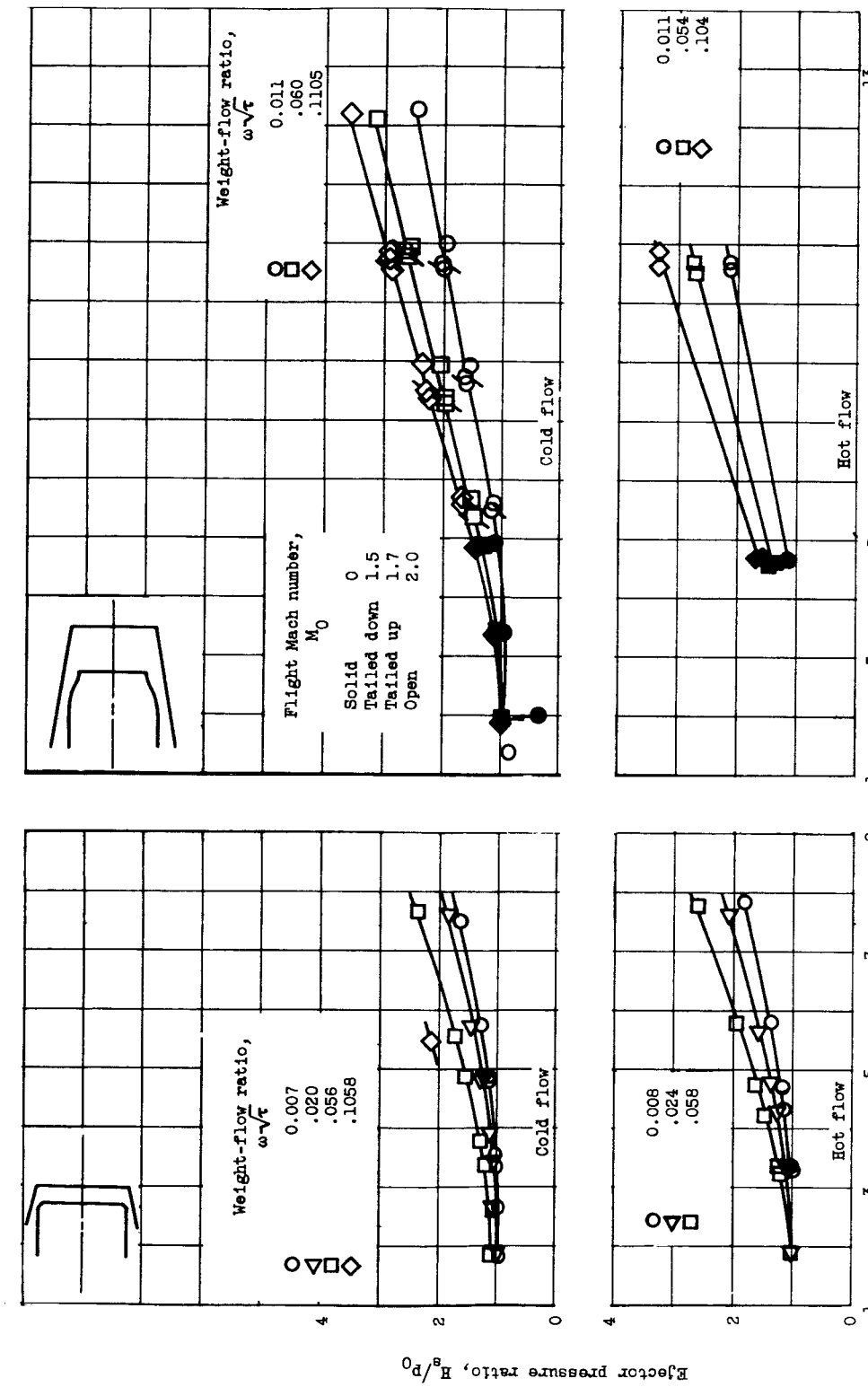

(c) Configuration A 1.13-0.23. Flight Mach numbers, 0, 0.62, and 1.5.

(d) Configuration A 1.24-0.70.

Figure 4. - Continued. Ejector pumping characteristics.

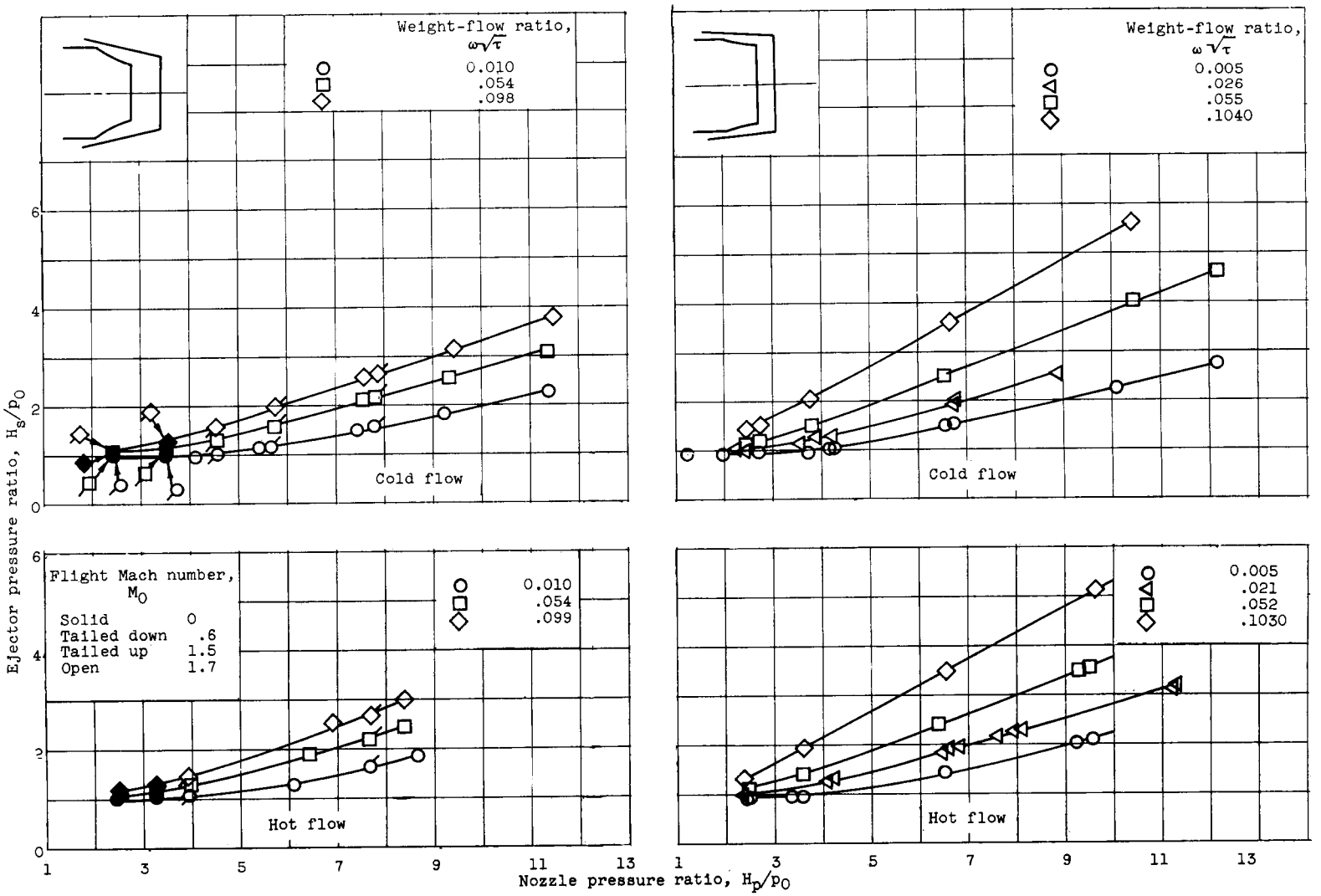

(e) Configuration B 1.16-0.494.

(f) Configuration B 1.14-0.214. Flight Mach numbers, 0, 0.62, 1.5, 1.7, and 2.0.

Figure 4. - Continued. Ejector pumping characteristics.

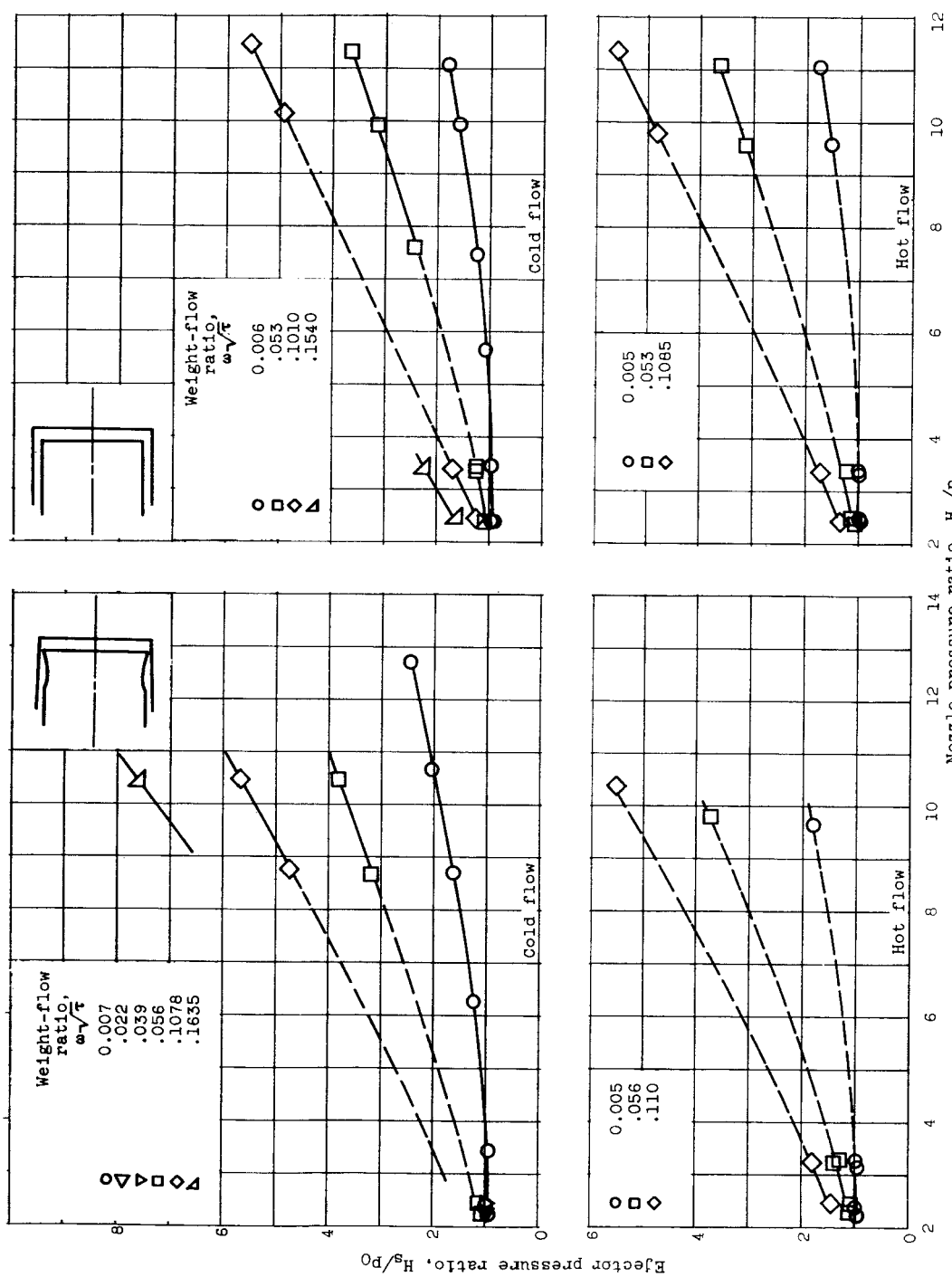

(g) Configuration B 1.12-0.123. Flight Mach numbers, 0, 0.57, and 2.0.

(h) Configuration B 1.16-0.133. Flight Mach numbers, 0, 0.56, and 1.7.

Figure 4. - Concluded. Ejector pumping characteristics.

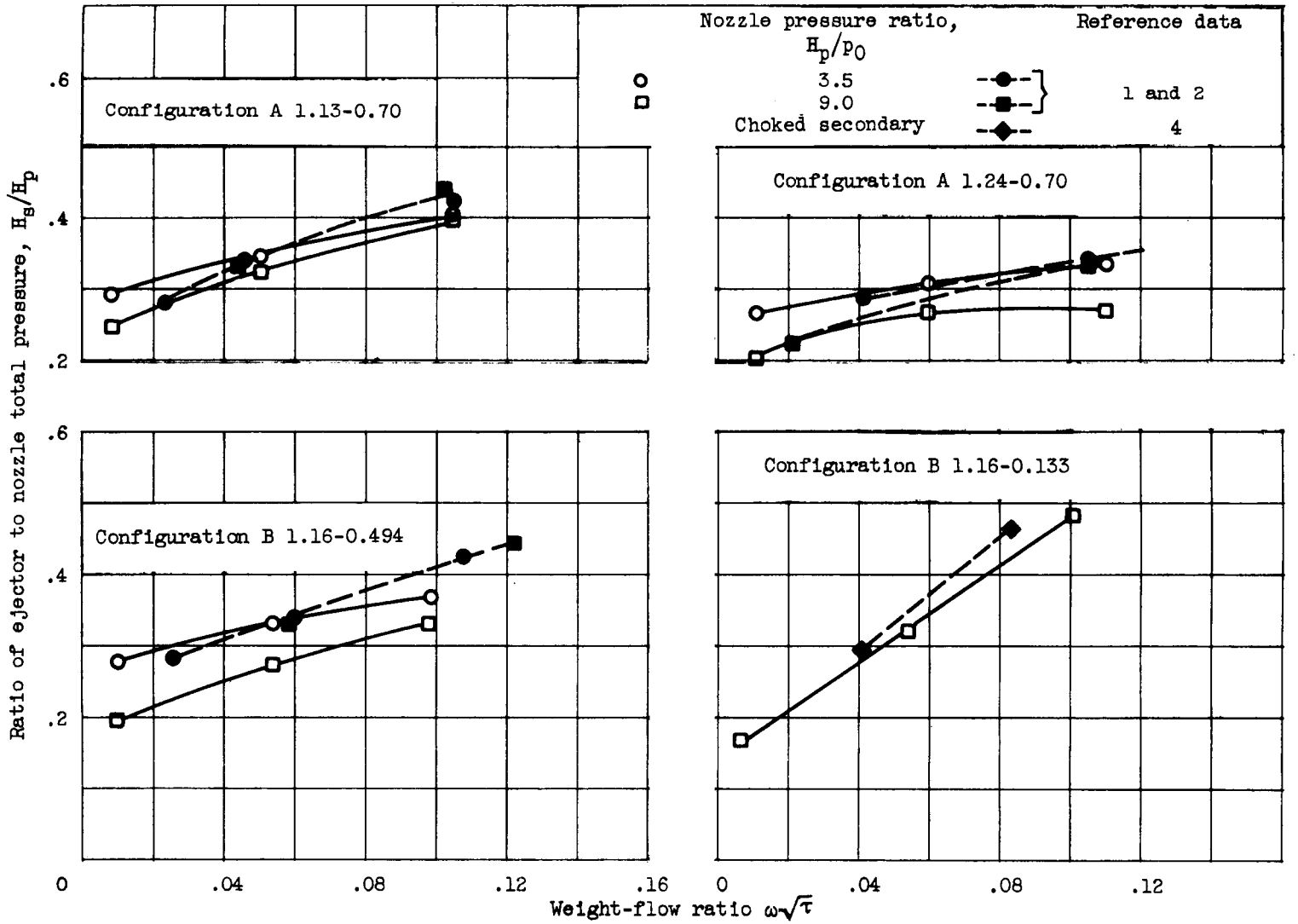

Figure 5. - Comparison of ejector pumping characteristics with results of references 1, 2, and 4. Cold flow.

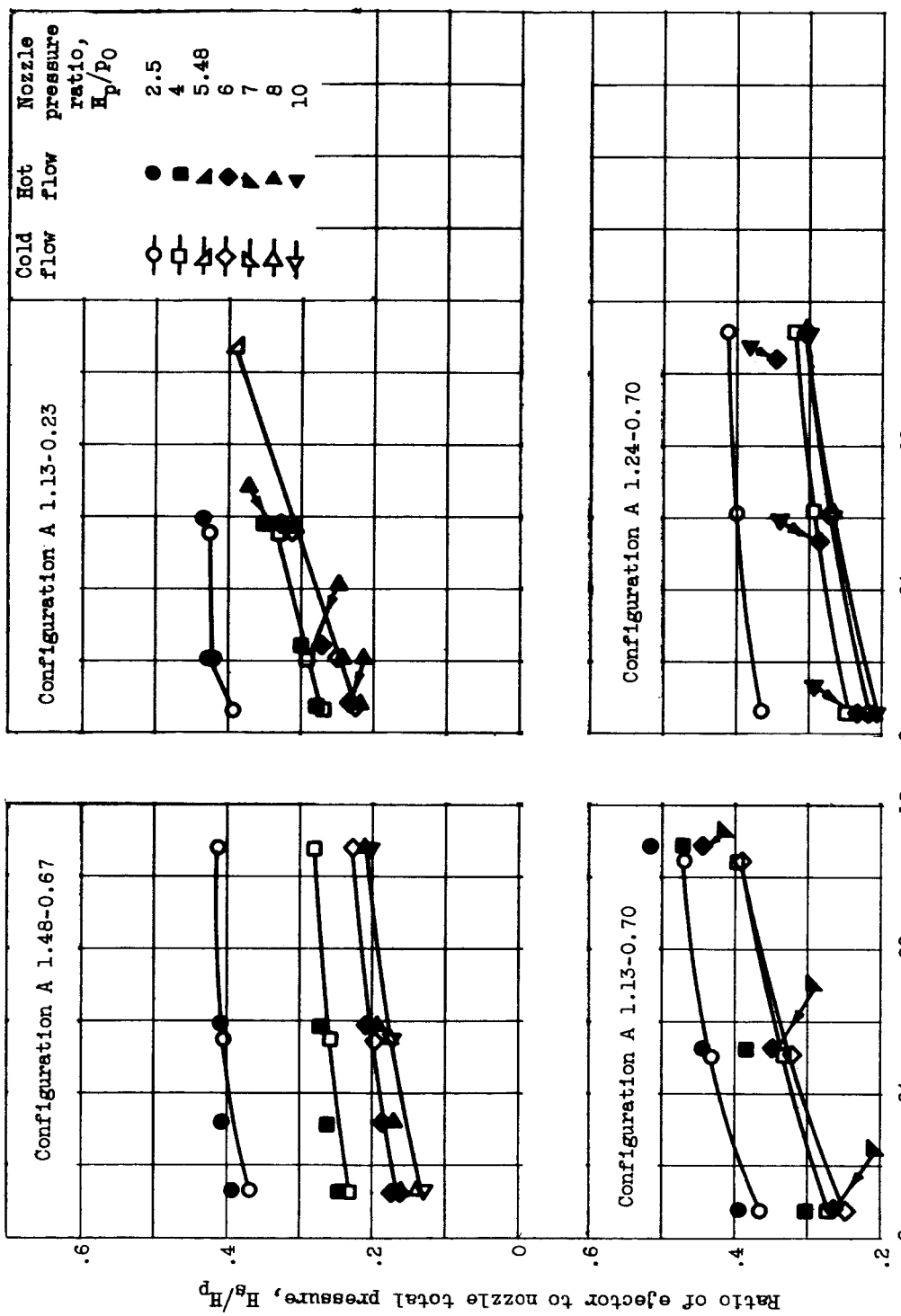

(a) Configuration A.

Figure 6. - Comparison of pumping characteristics for cold and hot flow.

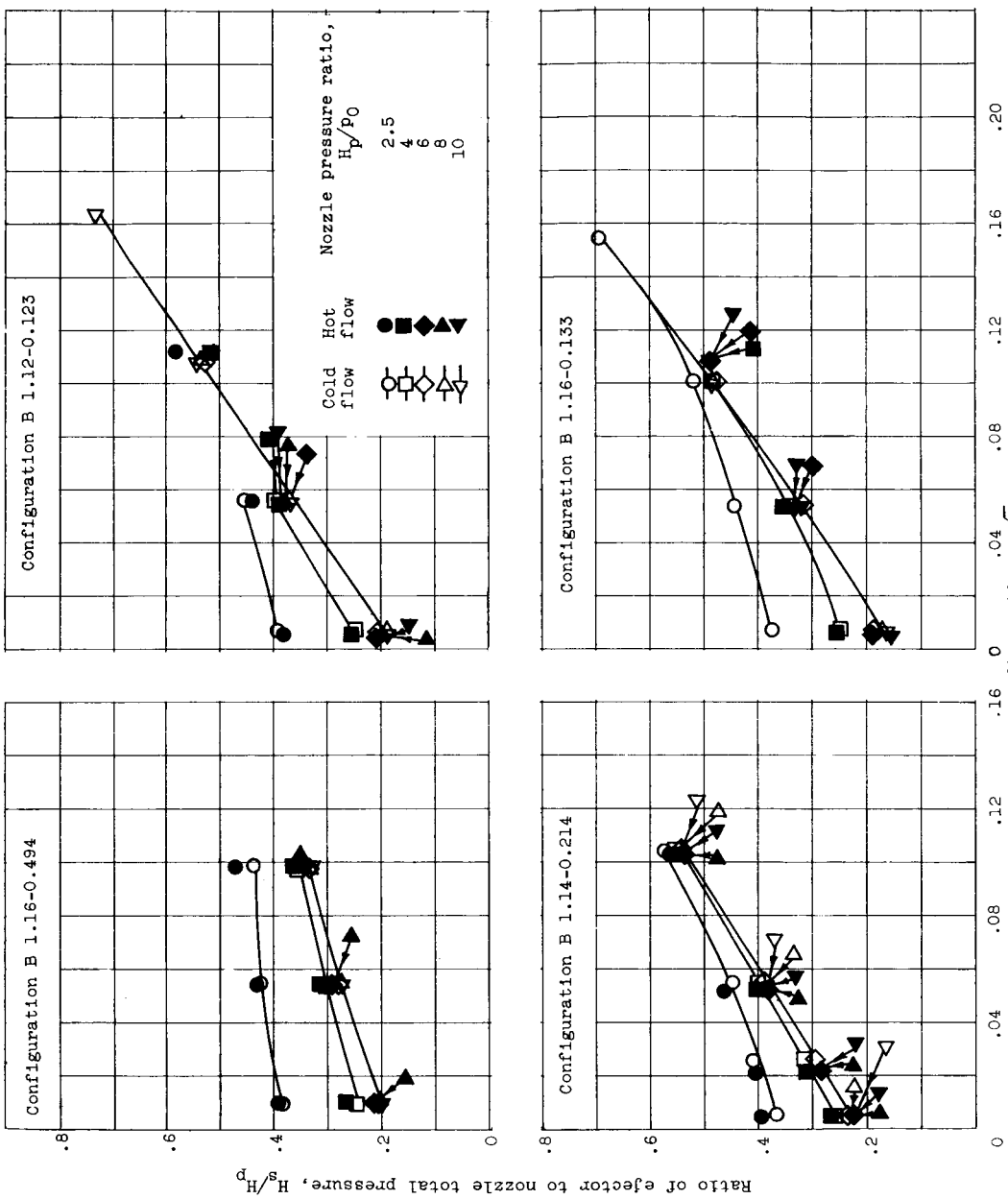

(b) Configuration B.

Figure 6. - Concluded. Comparison of pumping characteristics for cold and hot flow.

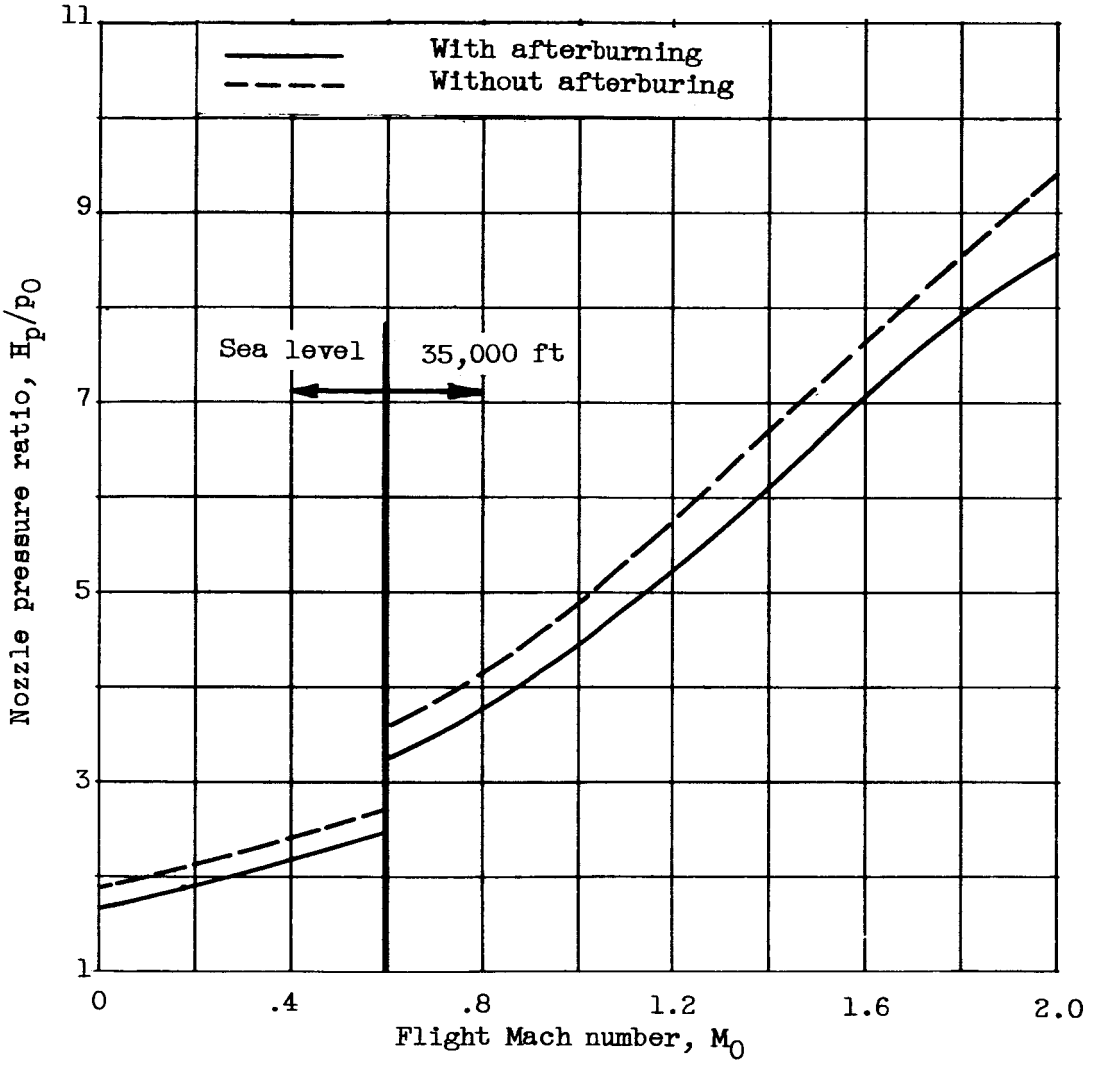

Figure 7. - Schedule of turbojet nozzle pressure ratio including estimated inlet pressure-recovery losses.

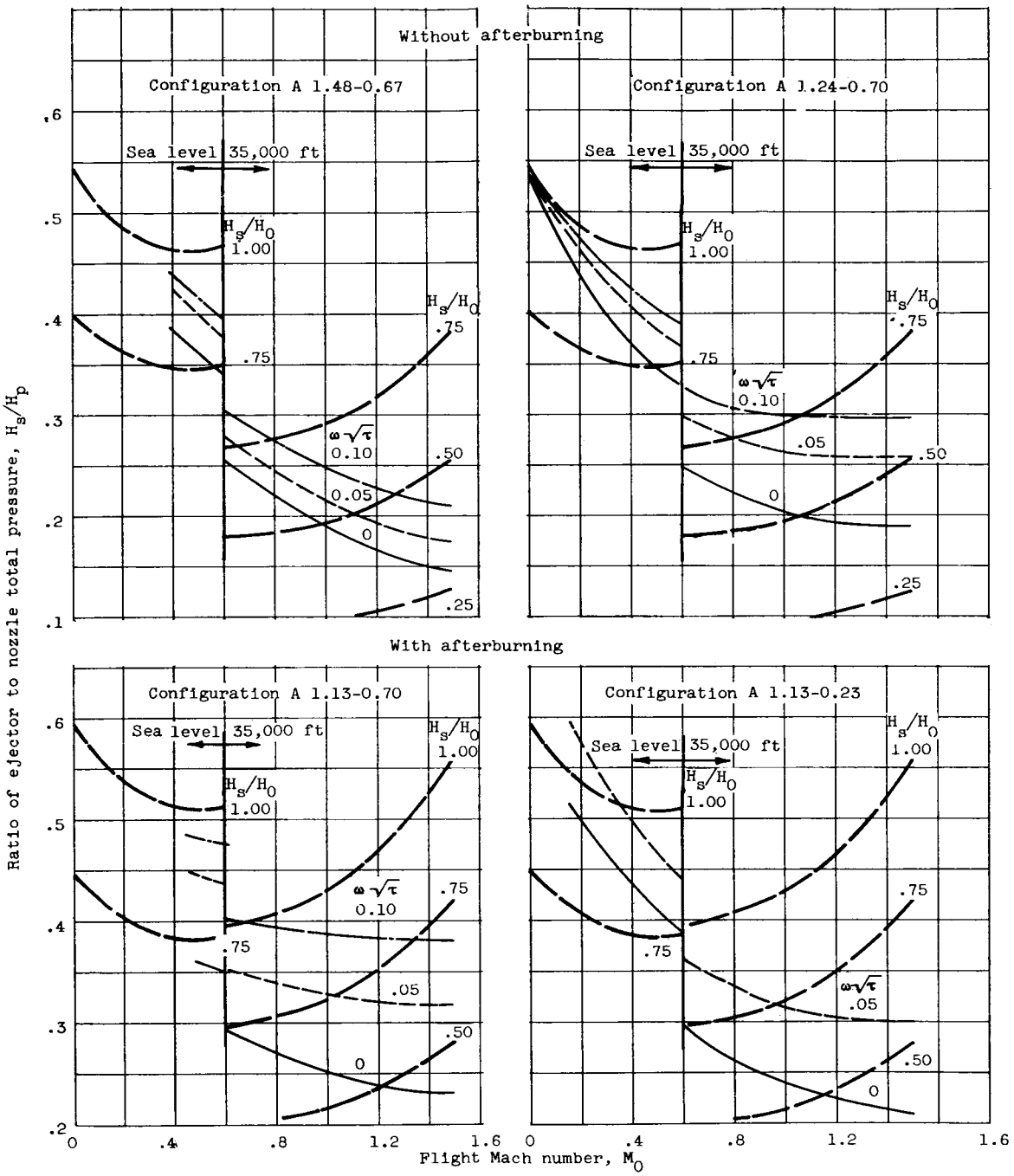

(a) Configuration A.

Figure 8. - Ejector air-supply requirements.

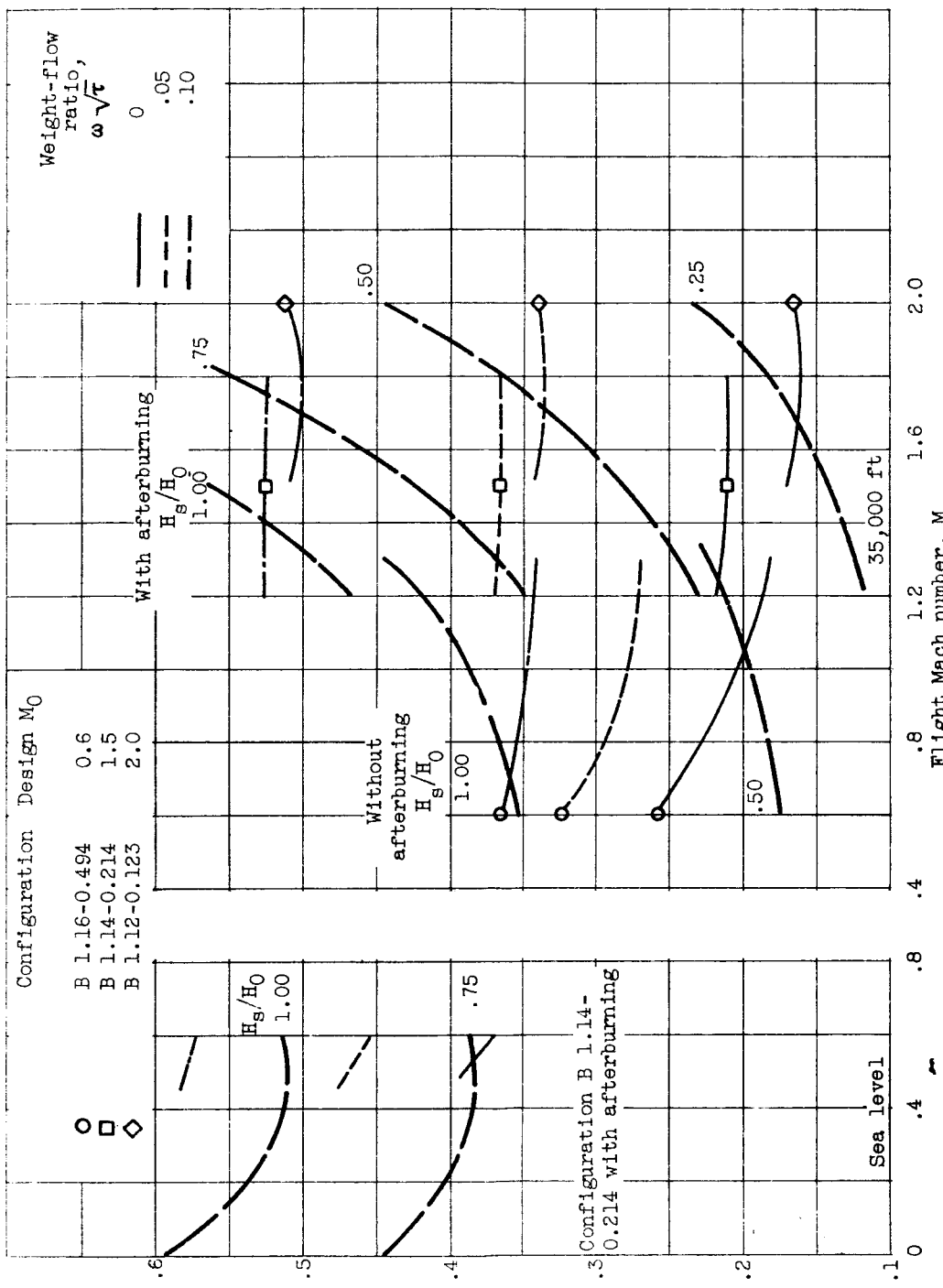

(b) Configuration B.

Figure 8. - Concluded. Ejector air-supply requirements.